



Research Article

Characterization and dye adsorption effectiveness of activated carbon synthesized from olive pomace

Fatma DENİZ¹, Öyküm BAŞGÖZ², Ömer GÜLER³, Mehmet Ali MAZMANCI¹

¹Department of Environmental Engineering, Mersin University, Mersin, Türkiye

²Department of Metallurgical and Material Engineering, Mersin University, Mersin, Türkiye

³Department of Machinery and Metal Technologies, Munzur University, Tunceli, Türkiye

ARTICLE INFO

Article history

Received: 18 August 2022

Revised: 23 November 2022

Accepted: 07 December 2022

Key words:

Activated carbon; Adsorption;
Aqueous solution; Dye
removing; Olive pomace

ABSTRACT

Studies, about products obtained from agricultural wastes, have increased within the scope of zero waste studies. The olive pomace is produced as a result of olive oil production. In the present study, activated carbon was synthesized using the olive pomace taken from the olive pomace processing plant operating with a three-phase process. The synthesized activated carbon characterization was performed using Scanning Electron Microscope (SEM), Fourier-Transform Infrared Spectroscopy (FT-IR), Brunauer – Emmett – Teller (BET), and X-Ray Crystallography (XRD) devices. Olive pomace activated carbon (OPAC) was used for the adsorption of dye from an aqueous solution. The adsorption efficiency of the OPAC was investigated. The initial pH value of dye solution (6–9), the amount of activated carbon (0.5 and 1.0 g/L), and initial dye concentration (600–1200 mg/L) were optimized. Also, adsorption kinetic and isotherm calculations were evaluated. The optimum parameters were found as the original pH value (pH=8) of dye solutions, OPAC amount of 1.0 g/L and the initial concentration of 1000 mg/L. The Langmuir isotherm model and the pseudo-second-order kinetic model were found as the most suitable models. It can be said that the synthesized material can be used at dye removing from wastewater.

Cite this article as: Deniz F, Başgöz Ö, Güler Ö, Mazmanlı MA. Characterization and dye adsorption effectiveness of activated carbon synthesized from olive pomace. Environ Res Tec 2022;5:4:369–379.

INTRODUCTION

The olive oil production is one of the important agro-industries [1]. There are 900 million olive trees on an area of approximately 10 million hectares in the world. According to the averages in last five seasons, olive oil production is around 2.91 million tons [2]. Olive oil production process

generates wastewater and pomace, which are difficult to treat. The amount and characteristics of wastes vary according to the production method. Two different processes, classical and continuous, are applied in olive oil production. In the classical production process, oil is extracted using hydraulic presses. Olives are washed with water, crushed and kneaded by adding water. The olive paste is then pressed

*Corresponding author.

*E-mail address: fatmadeniz@mersin.edu.tr



and oil, wastewater (black water) and solid phase (olive pomace) are separated. The continuous production process is based on the separation of the oil from the olive paste by centrifugation. It consists of feeding, washing, crushing and olive paste preparation units. Depending on the centrifuge used during production, there are two different processes: three-phase and two-phase. In the three-phase process, water is used. After the process, three phases are formed: oil, black water and olive pomace. Since process water is added, three times more wastewater is generated than in the conventional process. In the two-phase process, no process water is added. After the process, two phases are formed as oil and olive pomace. Black water is not formed. Most of the black water is in the pomace [3].

Pomace consists of olive, seed, and pulp. Approximately, 270 and 250 kg of anhydrous pomace is produced per ton of olive in two-phase and three-phase processes, respectively [4]. An average of 3.3 million tons of pomace waste in two-phase systems and 3.06 million tons in three-phase systems (at 5% humidity) are produced annually. The results show that every year a high amount of pomace is produced in the world. Pomace has been used to synthesize activated carbon after various processes to reuse. The effectiveness of olive pomace activated carbon (OPAC) in removing various pollutants such as cadmium II, chromium III, arsenic III, phenol, toluene, iodine, methylene blue, etc. from wastewater has been investigated [5]. Dyes are one of these pollutants. If the wastewater containing dye is discharged to the receiving environment without treatment, the dyes in the wastewater are also released to the receiving environment. Dyes are toxic to living organisms. Since it gives color to the water and prevents sunlight from entering the water, it hinders the vital activities of aquatic organisms. For this reason, discharging wastewater containing dye to receiving environments without treatment causes a critical environmental problem. Many studies have been carried out on treating wastewater containing dye [6–9]. Methods such as adsorption, sedimentation, filtration, coagulation, electrocoagulation, biodegradation, electrochemical oxidation, Fenton process, ozonation, sonolysis, wet air oxidation, electrical discharges, photocatalysis, photolysis were applied for the treatment of such wastewaters [6]. Among these methods, adsorption is an effective, simple, and frequently preferred purification technique [10]. The type of adsorbent and the method of synthesis of adsorbent affect the cost of adsorption processes. Activated carbon is generally used in adsorption processes for high porosity, sufficient pore size, large specific surface area, and high mechanical strength. These properties of activated carbon make it one of the reliable adsorbents since it provides a high-efficiency treatment of many organic and inorganic pollutants [11–14]. However, the high price of commercial activated carbons increases the cost of treatment. Therefore, agricultural wastes are used to synthesize the activated carbon for

reducing the cost [11]. There are studies in which agricultural wastes are used as activated carbon after various processes. Rice husk, citrus peel, eggshells, sawdust, cigarette waste, alfalfa, by-products from industries (e.g., sugar cane, paper, tea leaves, and others), palm tree cob, plum kernels, nutshell, wood, corn cob cottonseed shell, rubber seed shell, almond shell, coconut shell, bamboo powder, sunflower seed shell, peach kernel, and olive pomace can be given as examples of these agricultural wastes [11, 15]. These wastes are used as adsorbent to treat wastewater.

The aim of this study was to demonstrate the effectiveness of reusing an agricultural waste as an adsorbent in removing dye from an aqueous solution. OPAC synthesized from pomace was used as an adsorbent. The novelty of this study is that commercial dyes used at paper industry were studied.

EXPERIMENTAL

Carbonization Experiments

The olive pomace used in this study was taken from the three-phase pomace processing plant located in Mersin, Türkiye. The moisture content of olive pomace was calculated from the weight loss after drying at 103–105 °C for 3 hours and determined as 3.7%. Next, dried pomace (49.83 gr) was calcined in a specially produced metal screwed crucible at 800 °C for 1440 minutes using a muffle-type furnace.

The flow chart of the OPAC synthesis was given in Figure 1. It was determined that there was a weight loss of 21.41% in the pomace after the calcination process. Before the calcination process, as a result of the carbon-sulfur (Eltra CS-580) analysis, it was determined that the pomace contained 52.01% carbon and 0.025% sulfur. It was determined that the calcined pomace had 88.98% carbon and 0.038% sulfur.

Adsorption Experiments

Three different water-based dyes (DS-00102:WB dispensing yellow base: JR05 (DS-00102); DS-00203:WB dispensing orange base: JR05 (DS-00203); DS-00502:WB dispensing blue base: JR05 (DS-00502)) and the mixture of three water-based dyes solution (V: V: V; 1: 1: 1) were used. The dyes were taken from a cardboard factory in Mersin, Türkiye.

The pH, OPAC amount, and initial dye concentration effect were studied (Table 1). The sample volume was 200 mL. The original pH level of the aqueous solutions of the dyes was approximately 8. The pH values of solutions were adjusted using 0,1 and 0,01 M H₂SO₄ and NaOH solutions. OPAC was added to the samples after pH adjustment. The magnetic stirrer (at 150 rpm) was used for the mixing process, and samples were taken for color measurement at intervals of 15 minutes. Collected samples were centrifuged at 6000 rpm for 5 minutes for the color measurement of the supernatant. The color measurement was carried out using Hach Lange, DR3900 model spectrophotometer.

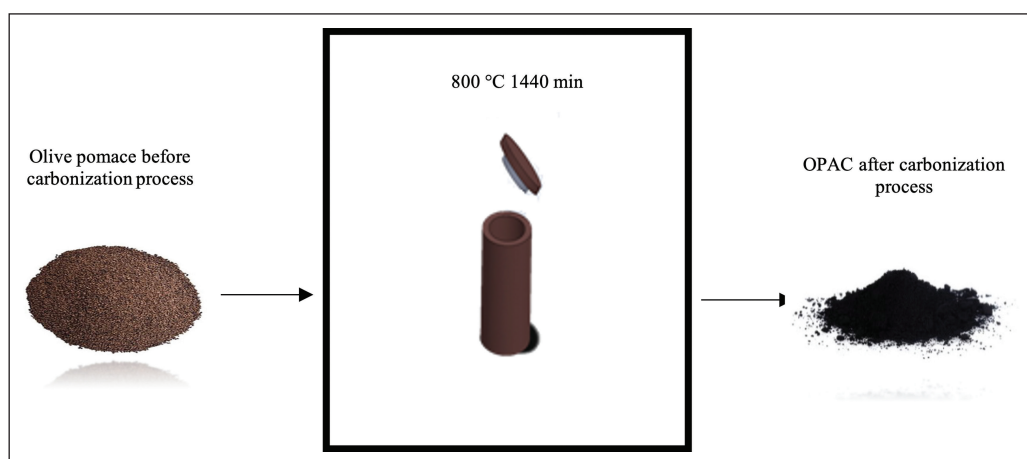


Figure 1. OPAC synthesis flow chart.

Table 1. Adsorption experiments conditions

	The effect of pH	The effect of OPAC amount
pH	6, 8*, 9	Optimum pH
AC amount (g AC/200 mL)	0,5	0.5, 1.0

*: Original pH value of aqueous solutions of dyes.

The dye removal efficiency was calculated using Equation 1.

$$Removal \% = \frac{C_0 - C_t}{C_0} \times 100 \quad (1)$$

where C_t (mg/L) is the concentration at t time, and C_0 (mg/L) is the initial concentration.

Isotherm (Langmuir and Freundlich) and kinetic models (pseudo-first and second order, and intraparticle diffusion) were calculated.

RESULTS AND DISCUSSION

Characterization of the OPAC

Structural properties of OPAC were analyzed with a Scanning Electron Microscope (SEM) (FEI-Quanta 650). Surface functional groups were investigated with Fourier Transform Infrared Spectrometer (FT-IR) (Jasco-6700). The surface area and pore volume of the OPAC were determined using The Brunauer – Emmett – Teller (BET) method by N_2 adsorption at $-196\text{ }^\circ\text{C}$ with surface area-pore size analyzer (Micrometrics Surface Area and Porosity-TriStar II). The structural feature of OPAC was examined by X-Ray Diffraction Measurement (XRD) (PANalytical-EMPYREAN) using Cu K α as a radiation source.

The SEM images of OPAC was given in Figure 2. The surface of the OPAC was smooth. This is the reason that total surface area was low as mentioned below. The sizes of the chars changed at wide range. Carbonization parameters such as the temperature, time and pressure affect the textur-

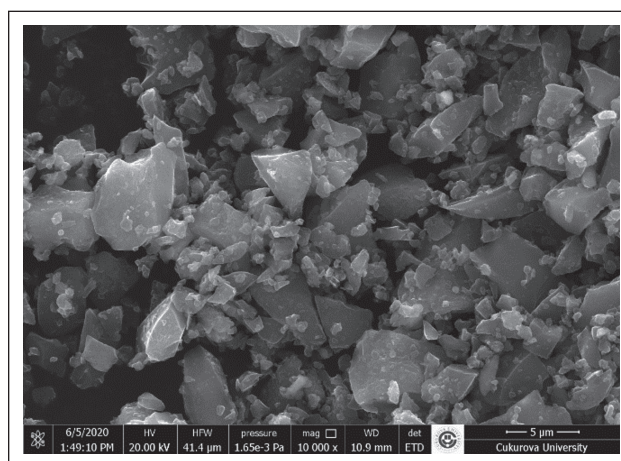


Figure 2. SEM images of OPAC.

al properties of synthesized material [16, 17]. At this study carbonization method was not optimized. The optimization of carbonization conditions can develop surface properties and adsorption capacity of material.

The FT-IR spectra for OPAC were shown in Figure 3. For the O-H bond of most carboxylic acids, a characteristic broad property is observed in the range $3300\text{--}2500\text{ cm}^{-1}$, with a secondary absorption close to 2600 cm^{-1} and overlapping the C-H stretching region [18]. Highly non-absorbent peaks above the region between 2700 and 2400 are not associated with any compound has multiple bounds. Hydride vibrations such as thiols and sulfides (SH), boranes (BH), phosphines (PH), silanes (SiH) and arsines (AsH) often cause these absorptions [18]. The peak at 2663 cm^{-1} is indicative for O-H stretching [19]. The peak at 2330 cm^{-1} can represent CO_2 [19]. The region between $2260\text{--}2100\text{ cm}^{-1}$ (2113 cm^{-1}) represents $C\equiv C$ stretch [18]. The peak at 1995 cm^{-1} may represent transition metal carbonyl that has the bands between $2100\text{--}1800\text{ cm}^{-1}$. The multi-bonded CO group gives an intense absorption band

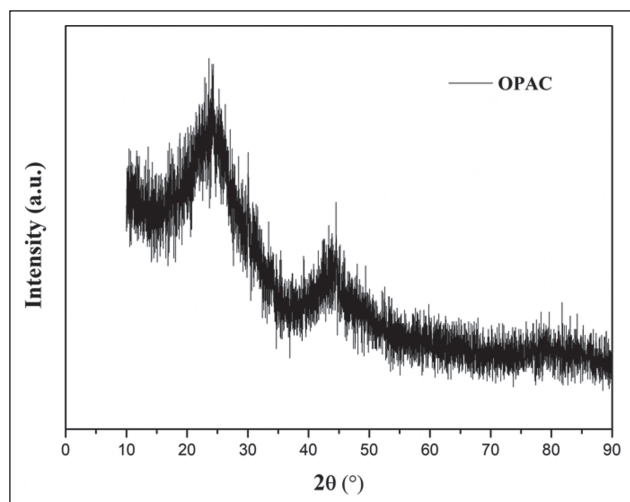


Figure 4. XRD plot of OPAC.

in regions close to 2000 cm^{-1} . The complexity and actual location of bands depend on the compounds nature [18]. C=O stretching vibrations at 1769 cm^{-1} peak represents of aldehydes, ketones, lactones or carboxyl groups [20]. Between $2000\text{--}1660\text{ cm}^{-1}$ is the aromatic combination in general [18]. Bands range between 1650 and 1750 cm^{-1} represent esterified and free carboxyl groups that may be convenient to identify pectins [21].

BET analysis results were given in Table 2. When the results were compared with other studies, it was seen that the calculated values for OPAC were lower [11, 12, 22]. It was thought that this situation was caused by the carbonization method applied. Temperature change, carbonization time, and used chemicals create differences in the surface properties of the obtained activated carbon [22].

XRD graph of OPAC was given in Figure 4. In the XRD graph, strong and weak peaks were observed at $2\theta=25^\circ$ and $2\theta=45^\circ$ respectively. The pores formed by the decomposition of carbon along the direction of the graphic structures form the peak at $2\theta=25^\circ$. This structure produces an more stable aromatic carbon than amorphous carbon [23, 24].

Table 2. Properties of OPAC

Total pore volume (cm^3/g)	Total pore area (m^2/g)	Surface area BET (m^2/g)
0,04976	26,962	17,5958

Adsorption Experiments

The Effect of Initial pH

One of the essential parameters in adsorption experiments is the pH value of solution [25]. The ionization degree of the pollutant compound and the adsorbent surface charge are affected by the pH of the solution [12, 26]. In addition, hydronium (H_3O^+) and hydroxide (OH^-) ions in the solution are adsorbed by the adsorbent, which affects the removal capacity of pollutants [27]. Researchers have studied the adsorption of various pollutants at pH ranging between 2–10.9 in different studies [5]. In this study, three initial pH values (6, 8, and 9) were studied. The experiments were performed at initial concentrations of 912, 820, and 996 mg/L for DS-00102, DS-00203, and DS-00502 dyes, respectively. Color removal findings for each sample were given in Figure 5.

Dye removal efficiencies of pH 6, 8, and 9 were close to each other for each dye. The maximum dye removal was carried out in the first 15 minutes. In the following minutes, the amount of dye remained at approximately the same values. The highest removal efficiencies for DS-00102, DS-00203, and DS-00502 dye solutions were calculated as 32, 37, and 55%, respectively.

The removal efficiencies obtained at pH 6, 8, and 9 indicate that dye removal can be done in this range. The different removal efficiencies for each dye were attributed to the differences in the dye surface load. Since pH 8 was the original pH, it was determined as the optimum pH value. Similar pH values (8.10–8.53) were studied by Pala et al. [28] for color removal. In addition, there are studies using similar [29, 30], acidic [12, 31], and basic [27, 30] pH values in adsorption studies with activated carbon obtained from olive pomace. The difference in pH is attributed to the difference in pollutants and carbonization methods.

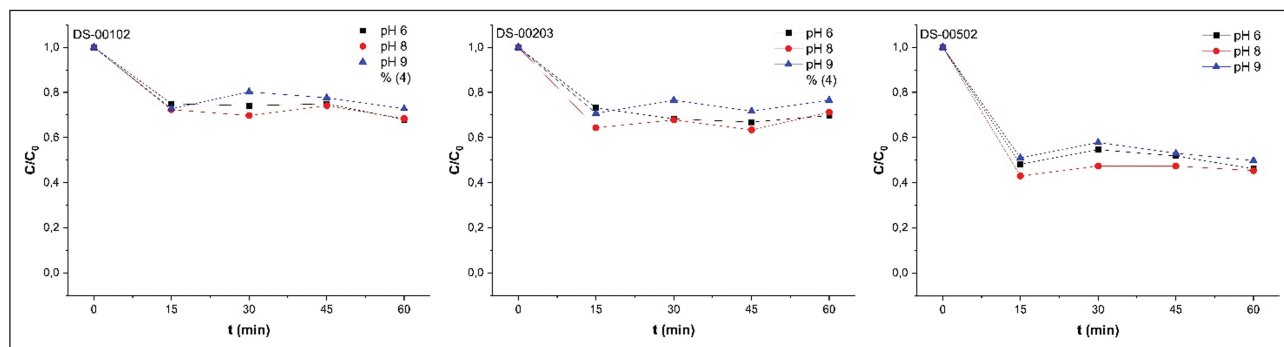


Figure 5. pH value optimization for color removal from DS-00102, DS-00203, and DS-00502 dye solutions (0.5 g OPAC/200 mL).

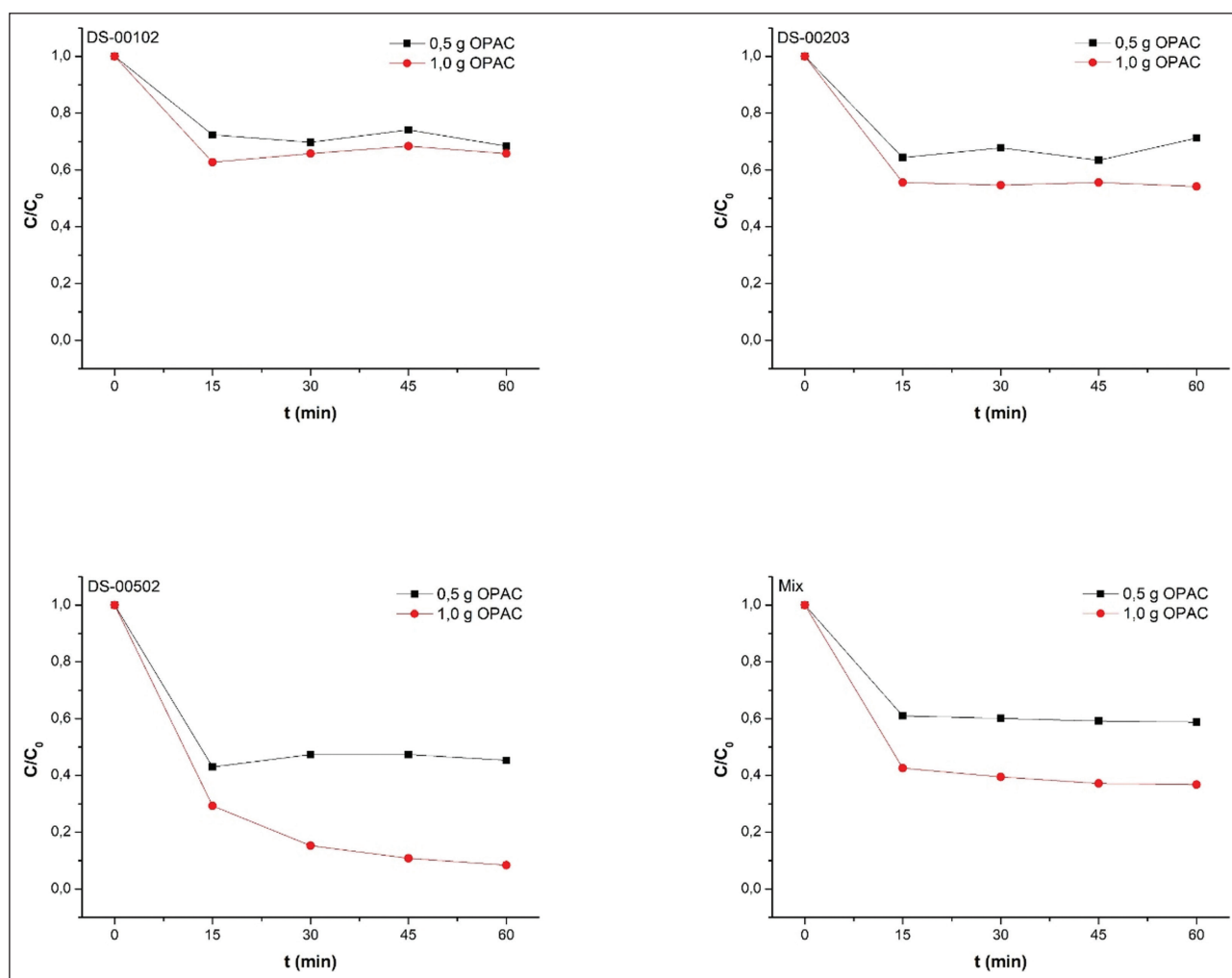


Figure 6. OPAC amount optimisation for colour removal from DS-00102, DS-00203, DS-00502, and mix dye solutions (pH=8).

The pH change was monitored during the experiment. After 60 minutes, the pH increased from 6 and 8 to 8.3 and 9.6, respectively.

The Effect of OPAC Amount

The experiments investigating the effect of OPAC amount (0.5 and 1.0 g/200 mL) were carried out at pH 8. The initial dye concentrations were 912, 820, 996, and 892 mg/L for the DS-00102, DS-00203, DS-00502, and mix samples (V: V; 1: 1: 1), respectively. Color removal efficiencies for different amounts of OPAC (0.5 and 1.0 g/200 mL dye solution) for each dye were given in Figure 6.

As the OPAC amount was increased from 0.5 g to 1.0 g, the color removal efficiency increased. The highest removal efficiencies with 1.0 g OPAC for DS-00102, DS-00203, DS-00502, and mixture samples were calculated as 37, 46, 92, and 63%, respectively. Among all dye solutions, the highest removal was achieved in DS-00502 (92%). Increasing the OPAC amount from 0.5 to 1.0 g increased the removing efficiency of the DS-00102 and DS-00203 dyes by 5 and 9%, re-

spectively. However, the increasing amount of OPAC in the DS-00502 dye solution increased the removal from 55% to 92%. Compared to previous studies, it was seen that higher removal efficiency was performed in a shorter time [5].

The Effect of Initial Dye Concentration

To examine the effect of initial dye concentration, DS-00502 dye solutions were prepared as 600, 800, 1000, and 1200 mg/L concentrations. OPAC (1.0 g/200 mL) was added to the solutions. Removal of 97, 93, 92 and 85% was obtained for 600, 800, 1000 and 1200 mg/L, respectively. When the initial dye concentration increased from 600 mg/L to 1200 mg/L, the adsorption capacity of OPAC increased from 110 to 207 mg/g. The highest dye removal was achieved at 1200 mg/L (1020 mg/L). If the remaining dye amount considered, the least amount of dye (18 mg/L) remained from initial concentration of 600 mg/L. However, the most effective removal was achieved with 1000 mg/L. In all experiments, 15 minutes was enough for the system to reach equilibrium. Time-dependent removal results were given in Figure 7.

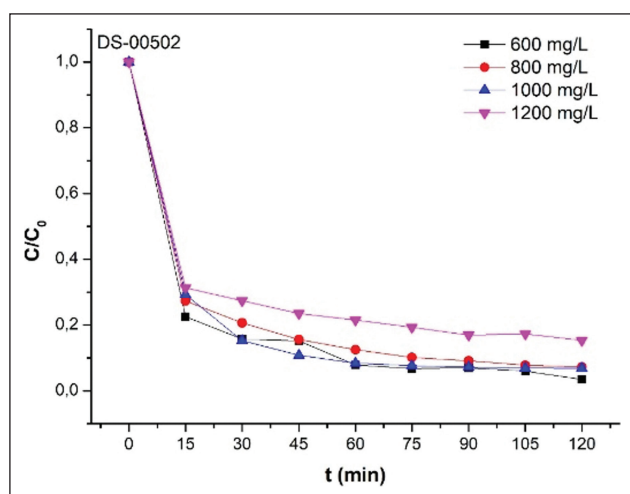


Figure 7. Initial dye concentration optimization for color removal from DS-00502 (pH=8 and 1.0 g OPAC /200 mL).

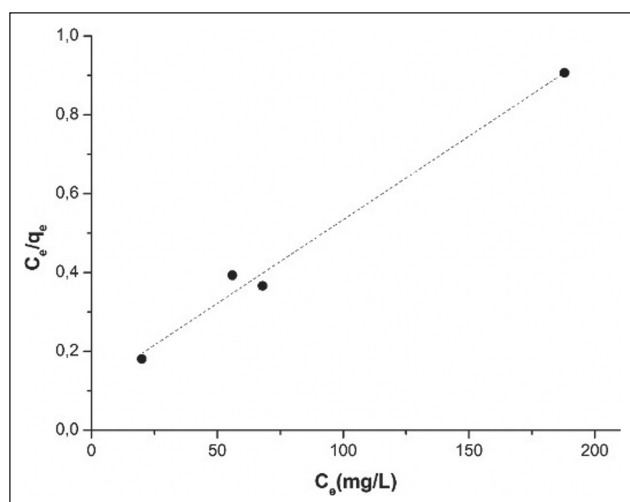


Figure 8. Langmuir isotherm curve.

For isotherm and kinetic calculations, DS-00502 dye solutions in four different initial concentrations (600, 800, 1000, and 1200 mg/L) were used. Experiment conditions were determined as pH 8, 1.0 g/200 mL OPAC and a reaction time of 120 minutes. The capacity of OPAC at equilibrium was calculated using Equation 2.

$$q_e = (C_0 - C_e)V/W \quad (2)$$

where C_e (mg/L) is the equilibrium concentration and C_0 is the initial concentration, W (g) OPAC amount and V (L) the sample volume. The capacity of OPAC at time t was calculated using Equation 3.

$$q_t = (C_0 - C_t)V/W \quad (3)$$

where C_t (mg/L) is the concentration at time t .

Adsorption Isotherms

Langmuir [32] and Freundlich [33] isotherms were calculated in this study.

Table 3. Parameters of isotherm models

q_{max} (mg/g)	Langmuir isotherm		Freundlich isotherm		
	R^2	K_L (L/mg)	n	R^2	K_F
238.09	0.9886	0.0382	3.4530	0.8877	47.5663

Table 4. The comparison of maximum adsorption capacity with previous studies

Activated carbon material	Removed pollutant	Max. adsorption capacity (mg/g)	References
This study	Dye	238.09	
Olive Stones	Phenol	58.8	[12]
Clay	Acid blue 29	104.83	
	Methylene blue	178.64	[17]
Olive Stone	Phenol	51	[31]
	Methylene blue	714	
Olive-seed waste residue	Methylene blue	263	[41]
Acorns		127	
Olive seeds	Methylene blue	115	[42]
Olive-waste cakes	Iodine	1495	[43]
	Methylene blue	490	

Langmuir isotherm states that the surface of the adsorbent has a certain number of active sites with the same energy, and the adsorption is reversible. According to this model, adsorption is limited to a single molecular layer [12]. Equilibrium is reached when the adsorption rate is equal to the desorption rate. The Langmuir isotherm accepts adsorption in a single layer, and the surface is homogeneous. It fills the homogeneous surface until the equilibrium moment. At equilibrium, the maximum amount of adsorption is reached [12, 34].

The Langmuir equation was given in Equation 4.

$$C_e/q_e = 1/(q_{max}K_L) + C_e/q_{max} \quad (4)$$

where K_L is the Langmuir constant and q_m (mg/g) is the maximum adsorption capacity of OPAC [35].

The graph of C_e versus C_e/q_e was given in Figure 8.

$1/q_{max}$ obtained from Figure 8 gives the slope [36]. Langmuir parameters were shown in Table 3.

Freundlich isotherm is applied to determine adsorption characteristics on heterogeneous surfaces [36]. Equations were given in Equations 5 and 6.

$$q_e = K_F C_e^{1/n} \quad (5)$$

$$\text{Log} q_e = \text{Log} K_F + 1/n \text{Log} C_e \quad (6)$$

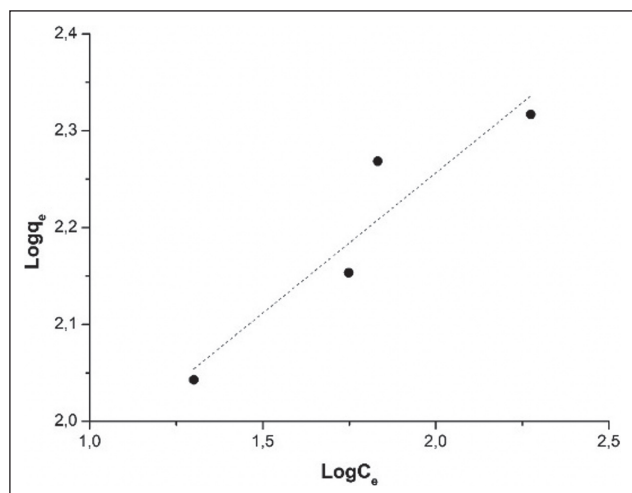


Figure 9. Freundlich isotherm curve.

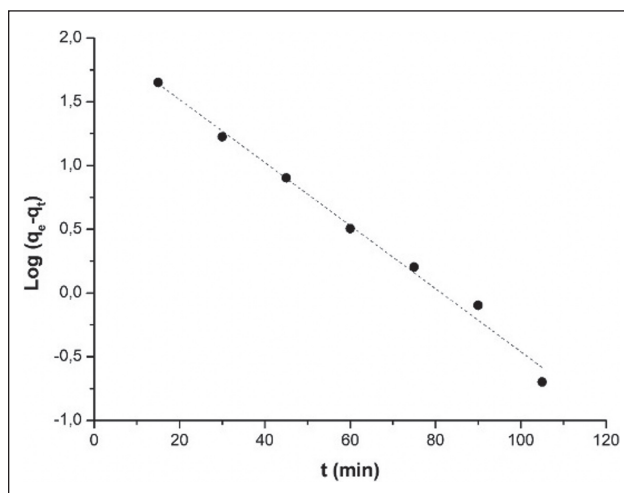


Figure 11. Pseudo-first-order curve.

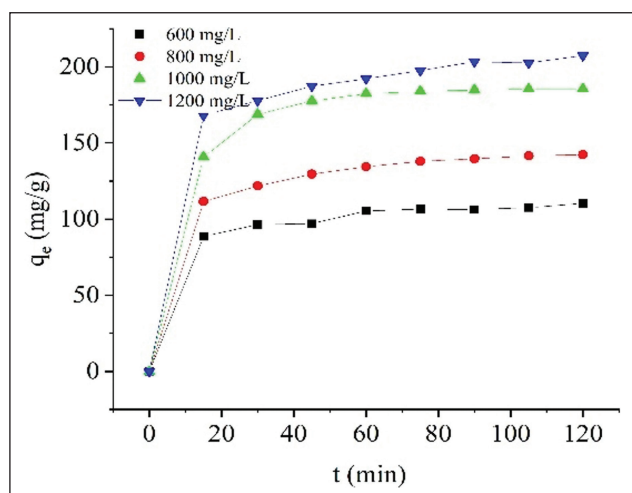


Figure 10. Adsorption capacities of OPAC.

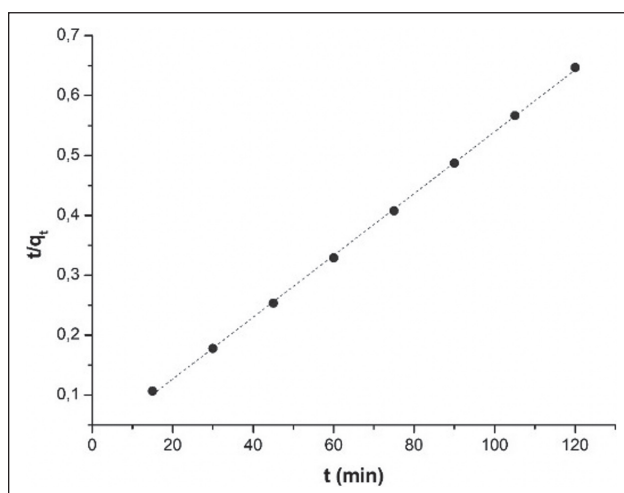


Figure 12. Pseudo-second-order curve.

where $1/n$ is heterogeneity factor and K_f (L/g) is the Freundlich constant [36].

The logarithmic form of Freundlich equation can be expressed as a line equation whose slope is $1/n$ and where it intersects the axis $\text{Log } K_f$ [12]. The graph of $\text{Log } C_e$ versus $\text{Log } q_e$ was given in Figure 9, and the parameters of the Freundlich isotherm were shown in Table 3.

The R^2 value obtained with the Langmuir isotherm is higher ($R^2=0.9886$) than Freundlich isotherm (Table 1). Adsorption occurs equally on the active sides of adsorbent, according to the Langmuir isotherm [37]. Similar findings were obtained in the color removal study of Pala et al. [28] and the phenol removal study of Bohli et al. [12].

The adsorption capacity of OPAC according to initial dye concentration was given in Figure 10. The maximum adsorption capacities were found as 110.4, 142.4, 185.6 and 207.4 for 600, 800, 1000 and 1200 mg/L initial dye concentrations, respectively. The results showed that the dye adsorption capacity in-

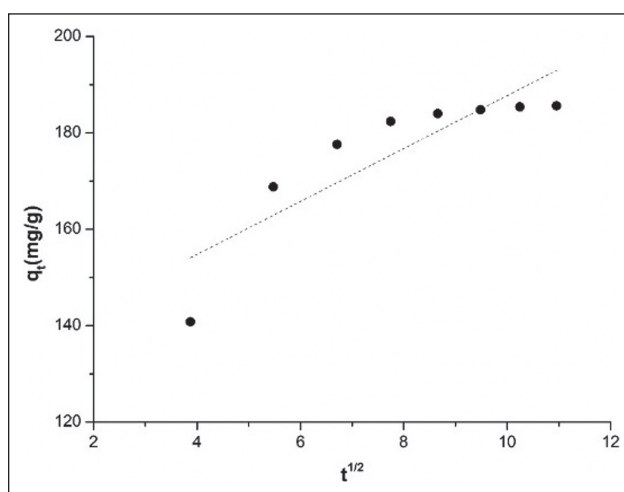


Figure 13. Intraparticle diffusion curve.

creased with increasing initial dye concentration. In Langmuir isotherm calculations, maximum adsorption capacity q_{max} was

Table 5. Parameters of kinetic models

Initial concentration (mg/L)	Pseudo-first-order				Pseudo-second-order				Intra particle diffusion	
	q_e (mg/g) cal.	q_e (mg/g) exp.	k_1 (min^{-1})	R^2	q_e (mg/g) cal.	q_e (mg/g) exp.	k_2 (min^{-1})	R^2	k_d (mg/g.min)	R^2
600	29.11	110.4	0.0237	0.9178	113.63	110.4	0.0015	0.9988	2.9485	0.9262
800	66.51	142.4	0.0382	0.9644	149.25	142.4	0.001	0.9997	4.3481	0.9506
1000	102.92	185.6	0.0568	0.9919	192.3	185.6	0.0011	0.9997	5.4924	0.7553
1200	63.22	207.4	0.0262	0.9492	217.39	207.4	0.0007	0.9991	5.5461	0.9810

found as 238.09 (Table 3). Adsorption isotherm models give the theoretical maximum adsorption capacity [38, 39]. OPAC did not reach the theoretical maximum adsorption capacity. It means that OPAC was not fully covered by dye and still has surface area for more adsorption [38, 40].

There are dye removal studies with similar q_{max} values [41]. In dye removal studies, methylene blue removal has been mostly studied. The maximum adsorption capacities of other studies were shown Table 4. The removal capacities of activated carbon can be different according to some properties or conditions such as used material, carbonization temperature, carbonization time, removed pollutant, initial dye concentration, initial pH, surface area of activated carbon, the amount of activated carbon, etc.

Adsorption Kinetics

Pseudo-first and second-order, and intraparticle diffusion model kinetic parameters were calculated.

According to Lagergren, the rate of adsorption is directly proportional to the number of pores on the adsorbent surface. The equation that gives the relation between adsorption capacity and contact time was given in Equation 7 [44].

$$\text{Log}(q_e - q_t) = \text{Log } q_e - k_1 \times t / 2.303 \quad (7)$$

where k_1 (min^{-1}) is the pseudo-first-order rate constant. The parameters were calculated using the graph of $\text{Log}(q_e - q_t)$ versus t [34]. The pseudo-first-order curve was given in Figure 11. The parameters were shown in Table 5.

According to pseudo-second-order model, valence forces are formed by exchanging electrons or joint use of electrons between adsorbent and adsorbate during adsorption [34, 45].

Calculations were made according to Equation 8.

$$t/q = 1/K_2 q_e^2 + (1/q_e) t \quad (8)$$

where K_2 (min^{-1}) refers to the pseudo-second-order rate constant. The parameters were calculated using the graph of t/q versus t (Fig. 12) and shown in Table 5.

The kinetic model defined by Weber was applied to evaluate

the diffusion mechanism and speed control steps [46]. The intraparticle diffusion kinetic equation was given in Equation 9.

$$q_t = k_d t^{1/2} + C \quad (9)$$

where C (mg/g) is the constant depending on the boundary layer thickness and k_d (mg/g.min) is the intraparticle diffusion rate constant [47].

Boundary layer diffusion occurs in the first few minutes, and intraparticle diffusion occurs in the time left. The step determining the adsorption rate is intraparticle diffusion [48]. The q_t versus $t^{1/2}$ was drawn to determine the effect of intraparticle diffusion (Fig. 13). The slope of the obtained equation gives the velocity constant [49, 50]. An intraparticle diffusion plot was drawn using the data obtained after the 15th minute.

Results showed that R^2 value closest to 1 were obtained with pseudo-second-order kinetic. Therefore, the adsorption was carried out by the pseudo-second-order kinetic.

CONCLUSIONS

Activated carbon was synthesized from the pomace obtained by the three-phase process. Synthesized activated carbon was used to adsorption four different dyes (DS-00102, DS-00203, DS-00502, and mix) from the aqueous solution. The pH value of dye solution, the amount of activated carbon, and the initial dye concentration parameters were optimized. Adsorption kinetics and isotherm models were compared. The most effective removal (92%) was obtained in DS-00502 dye. The optimum parameters were the original pH value (pH=8), 1.0 g/L OPAC, 1000 mg/L initial concentration. The Langmuir isotherm and pseudo-second-order kinetic have been found as the most suitable models. As a result, it can be said that the synthesized material can be used at dye removing from wastewater.

ACKNOWLEDGMENT

The authors thank the Mersin University Scientific Research Projects Department to provide the financial support (Project Number: 2015-AP4-1368).

DATA AVAILABILITY STATEMENT

The authors confirm that the data that supports the findings of this study are available within the article. Raw data that support the finding of this study are available from the corresponding author, upon reasonable request.

CONFLICT OF INTEREST

The authors declared no potential conflicts of interest with respect to the research, authorship, and/or publication of this article.

ETHICS

There are no ethical issues with the publication of this manuscript.

REFERENCES

- [1] N. Gholamzadeh, M. Peyravi, and M. Jahanshahi, "Study on olive oil wastewater treatment: Nanotechnology impact," *Journal of Water and Environmental Nanotechnology*, Vol. 1, pp. 145-161, 2016.
- [2] Republic of Turkey Ministry of Trade, "2019 olive and olive oil report," Republic of Turkey Ministry of Trade, Turkey, 2020.
- [3] F. Şengül, A. Özer, E. Çatalkaya, E. Oktav, H. Evcil, O. Çolak, and Y. Sağer, "A project on the purification of olive processing waste," T. C. Dokuz Eylül University, Engineering Faculty, Department of Environment Engineering, 2003. [Turkish]
- [4] Republic of Turkey Ministry of Trade, "Comparison of olive oil production processes," Republic of Turkey Ministry of Environment and Urbanization Turkey, 2020.
- [5] J. Saleem, U. B. Shahid, M. Hijab, H. Mackey, and G. McKay, "Production and applications of activated carbons as adsorbents from olive stones," *Biomass Conversion and Biorefinery*, pp. 1–28, 2019. [CrossRef]
- [6] C. Fernández, M. S. Larrechi, and M. P. Callao, "An analytical overview of processes for removing organic dyes from wastewater effluents," *TrAC Trends in Analytical Chemistry*, Vol. 29, pp. 1202–1211, 2010. [CrossRef]
- [7] S. Ahmed, S. Aktar, S. Zaman, R. A. Jahan, and M. L. Bari, "Use of natural bio-sorbent in removing dye, heavy metal and antibiotic-resistant bacteria from industrial wastewater," *Applied Water Science*, Vol. 10, pp. 1–10, 2020. [CrossRef]
- [8] V. Selen and Ö. Güler, "Modeling of congo red adsorption onto multi-walled carbon nanotubes using response surface methodology: Kinetic, isotherm and thermodynamic studies," *Arabian Journal for Science and Engineering*, Vol. 46, pp. 6579–6592, 2021. [CrossRef]
- [9] V. D. Pakhale and P.R. Gogate, "Removal of rhodamine 6g from industrial wastewater using combination approach of adsorption followed by sonication," *Arabian Journal for Science and Engineering*, Vol. 46, pp. 6473–6484, 2021. [CrossRef]
- [10] M. Bahrami, M. Amiri, and F. Bagheri, "Optimization of crystal violet adsorption by chemically modified potato starch using response surface methodology," *Pollution*, Vol. 6, pp. 159–170, 2020.
- [11] M. Berrios, M. A. Martin, and A. Martin, "Treatment of pollutants in wastewater: Adsorption of methylene blue onto olive-based activated carbon," *Journal of Industrial and Engineering Chemistry*, Vol. 18, pp. 780–784, 2012. [CrossRef]
- [12] T. Bohli, N. Fiol Santaló, I. Villaescusa Gil, and A. Ouederni, "Adsorption on activated carbon from olive stones: Kinetics and equilibrium of phenol removal from aqueous solution," *Journal of Chemical Engineering and Process Technology*, Vol. 4, pp. 165, 2013.
- [13] M. Uğurlu, A. Gürses, and M. Açıkıldız, "Comparison of textile dyeing effluent adsorption on commercial activated carbon and activated carbon prepared from olive stone by ZnCl₂ activation," *Microporous and Mesoporous Materials*, Vol. 111, pp. 228–235, 2008. [CrossRef]
- [14] K. Mohanty, D. Das, and M. Biswas, "Adsorption of phenol from aqueous solutions using activated carbons prepared from tectona grandis sawdust by ZnCl₂ activation," *Chemical Engineering Journal*, Vol. 115, pp. 121-131, 2005. [CrossRef]
- [15] N. Hossain, M.A. Bhuiyan, B.K. Pramanik, S. Nizamuddin, and G. Griffin, "Waste materials for wastewater treatment and waste adsorbents for bio-fuel and cement supplement applications: A critical review," *Journal of Cleaner Production*, Vol. 255, pp. Article 120261, 2020. [CrossRef]
- [16] N. Howaniec, "Olive pomace-derived carbon materials—effect of carbonization pressure under CO₂ atmosphere," *Materials*, Vol. 12, Article 2872, 2019. [CrossRef]
- [17] F. Marrakchi, M. Bouaziz, and B. Hameed, "Activated carbon–clay composite as an effective adsorbent from the spent bleaching sorbent of olive pomace oil: Process optimization and adsorption of acid blue 29 and methylene blue," *Chemical Engineering Research and Design*, Vol. 128, pp. 221–230, 2017. [CrossRef]
- [18] J. Coates. "Interpretation of infrared spectra, a practical approach," John Wiley & Sons, Inc., Newtown, USA, 2006. [CrossRef]
- [19] R. Rotaru, P. Samoila, N. Lupu, M. Grigoras, and V. Harabagiu, "Ferromagnetic materials obtained through ultrasonication. 1. Maghemite/goethite nanocomposites," *Revue Roumaine de Chimie*, Vol. 2017, pp. 131–138, 2017.

- [20] S. M. Yakout and G. Sharaf El-Deen, "Characterization of activated carbon prepared by phosphoric acid activation of olive stones," *Arabian Journal of Chemistry*, Vol. 9(Suppl 2), pp. S1155–S1162, 2011. [CrossRef]
- [21] H. Arslanoglu, H. Altundogan, and F. Tumen, "Preparation of cation exchanger from lemon and sorption of divalent heavy metals," *Bioresource Technology*, Vol. 99, pp. 2699–2705, 2008. [CrossRef]
- [22] I. H. Aljundi and N. Jarrah, "A study of characteristics of activated carbon produced from Jordanian olive cake," *Journal of Analytical and Applied Pyrolysis*, Vol. 81, pp. 33–36, 2008. [CrossRef]
- [23] L. J. Kennedy, J. J. Vijaya, and G. Sekaran, "Effect of two-stage process on the preparation and characterization of porous carbon composite from rice husk by phosphoric acid activation," *Industrial & Engineering Chemistry Research*, Vol. 43, pp. 1832–1838, 2004. [CrossRef]
- [24] T.-H. Liou, "Development of mesoporous structure and high adsorption capacity of biomass-based activated carbon by phosphoric acid and zinc chloride activation," *Chemical Engineering Journal*, Vol. 158, pp. 129–142, 2010. [CrossRef]
- [25] E. I. Ugwu, and J. C. Agunwamba, "A review on the applicability of activated carbon derived from plant biomass in adsorption of chromium, copper, and zinc from industrial wastewater," *Environmental Monitoring and Assessment*, Vol. 192, pp. 1–12, 2020. [CrossRef]
- [26] A. Maleki, A. Mahvi, R. Ebrahimi, and K. Jamil, "Evaluation of barley straw and its ash in removal of phenol from aqueous system," *World Applied Sciences Journal*, Vol. 8, pp. 369–373, 2010.
- [27] M. Bahrami, M.J. Amiri, and F. Bagheri, "Optimization of the lead removal from aqueous solution using two starch based adsorbents: Design of experiments using response surface methodology (RSM)," *Journal of Environmental Chemical Engineering*, Vol. 7, Article 102793, 2019. [CrossRef]
- [28] A. Pala, P. Galiatsatou, E. Tokat, H. Erkaya, C. Israilides, and D. Arapoglou, "The use of activated carbon from olive oil mill residue, for the removal of colour from textile wastewater," *European Water*, Vol. 13, pp. 29–34, 2006.
- [29] G. Cimino, R. Cappello, C. Caristi, and G. Toscano, "Characterization of carbons from olive cake by sorption of wastewater pollutants," *Chemosphere*, Vol. 61, pp. 947–955, 2005. [CrossRef]
- [30] A. Türkyılmaz, and K. Işınkaralar, "Removal of antibiotics (tetracycline and penicillin G) from water solutions by adsorption on activated carbon," *Journal of Engineering Sciences and Design*, Vol. 8, pp. 943–951, 2020.
- [31] N. Soudani, S. Souissi-najar, and A. Ouederni, "Influence of nitric acid concentration on characteristics of olive stone based activated carbon," *Chinese Journal of Chemical Engineering*, Vol. 21, pp. 1425–1430, 2013. [CrossRef]
- [32] I. Langmuir, "The adsorption of gases on plane surfaces of glass, mica and platinum," *Journal of the American Chemical Society*, Vol. 40, pp. 1361–1403, 1918. [CrossRef]
- [33] H. Freundlich, "Über die adsorption in lösungen," *Zeitschrift für physikalische Chemie*, Vol. 57, pp. 385–470, 1907. [Deutsch] [CrossRef]
- [34] N. Abdel-Ghani, E. Rawash, and G. El-Chaghaby, "Equilibrium and kinetic study for the adsorption of p-nitrophenol from wastewater using olive cake based activated carbon," *Global Journal of Environmental Science and Management*, Vol. 2, pp. 11, 2016.
- [35] J.-J. Gao, Y.-B. Qin, T. Zhou, D.-D. Cao, P. Xu, D. Hochstetter, and Y.-F. Wang, "Adsorption of methylene blue onto activated carbon produced from tea (*Camellia sinensis* L.) seed shells: Kinetics, equilibrium, and thermodynamics studies," *Journal of Zhejiang University Science B*, Vol. 14, pp. 650–658, 2013. [CrossRef]
- [36] G. Vijayakumar, R. Tamilarasan, and M. Dharmendirakumar, "Adsorption, kinetic, equilibrium and thermodynamic studies on the removal of basic dye rhodamine-b from aqueous solution by the use of natural adsorbent perlite," *Journal of Materials and Environmental Science*, Vol. 3, pp. 157–170, 2012.
- [37] E. Musin, "Adsorption modelling," *Environmental Engineerin Thesis*, Mikkeli University of Applied Sciences, Finland, 2013.
- [38] I. Anastopoulos, and G. Z. Kyzas, "Agricultural peels for dye adsorption: A review of recent literature," *Journal of Molecular Liquids*, Vol. 200, pp. 381–389, 2014. [CrossRef]
- [39] K. Bharathi and S. Ramesh, "Removal of dyes using agricultural waste as low-cost adsorbents: A review," *Applied Water Science*, Vol. 3, pp. 773–790, 2013. [CrossRef]
- [40] O. Lawas, A. Sanni, I. Ajayi, and O. Rabi, "Equilibrium, thermodynamic and kinetic studies for the biosorption of aqueous lead (ii) ions onto the seed husk of *Calophyllum inophyllum*," *Journal of Hazardous Materials*, Vol. 177, pp. 829–835, 2010. [CrossRef]
- [41] G. Stavropoulos, and A. Zabaniotou, "Production and characterization of activated carbons from olive-seed waste residue," *Microporous and Mesoporous Materials*, Vol. 82, pp. 79–85, 2005. [CrossRef]
- [42] W. K. Lafi, "Production of activated carbon from acorns and olive seeds," *Biomass and Bioenergy*, Vol. 20, pp. 57–62, 2001. [CrossRef]

- [43] A. Baçaoui, A. Yaacoubi, A. Dahbi, C. Bennouna, R. P. T. Luu, F. Maldonado-Hodar, J. Rivera-Utrilla, and C. Moreno-Castilla, "Optimization of conditions for the preparation of activated carbons from olive-waste cakes," *Carbon*, Vol. 39, pp. 425–432, 2001. [\[CrossRef\]](#)
- [44] S. Lagergren, "Zur theorie der sogenannten adsorption gelöster stoffe, kungliga svenska vetenskap-sakademiens," *Handlingar*, Vol. 24, pp. 1–39, 1898. [Deutsch]
- [45] S. Deng, R. Ma, Q. Yu, J. Huang, and G. Yu, "Enhanced removal of pentachlorophenol and 2, 4-d from aqueous solution by an aminated biosorbent," *Journal of Hazardous Materials*, Vol. 165, pp. 408–414, 2009. [\[CrossRef\]](#)
- [46] W. J. Weber, and J. C. Morris, "Kinetics of adsorption on carbon from solution," *Journal of the sanitary engineering division*, Vol. 89, pp. 31–60, 1963. [\[CrossRef\]](#)
- [47] T. A. Saleh, M. N. Siddiqui, and A. A. Al-Arfaj, "Kinetic and intraparticle diffusion studies of carbon nanotubes-titania for desulfurization of fuels," *Petroleum Science and Technology*, Vol. 34, pp. 1468–1474, 2016. [\[CrossRef\]](#)
- [48] O. Keskinan, M. Z. L. Goksu, A. Yuceer, M. Başibüyük, and C. F. Forster, "Heavy metal adsorption characteristics of a submerged aquatic plant (*myriophyllum spicatum*)," *Process Biochemistry*, Vol. 39, pp. 179–183, 2003. [\[CrossRef\]](#)
- [49] P. Waranusantigul, P. Pokethitiyook, M. Kruatrachue, and E. Upatham, "Kinetics of basic dye (methylene blue) biosorption by giant duckweed (*spirodela polyrrhiza*)," *Environmental Pollution*, Vol. 125, pp. 385–392, 2003. [\[CrossRef\]](#)
- [50] P. Ramachandran, R. Vairamuthu, and S. Pon-nusamy, "Adsorption isotherms, kinetics, thermodynamics and desorption studies of reactive orange 16 on activated carbon derived from ananas comosus (l.) carbon," *Journal of Engineering and Applied Sciences*, Vol. 6, pp. 15–26, 2011.